Cerebral Cortex, March 2020;30: 913–928

doi: 10.1093/cercor/bhz136
Advance Access Publication Date: 11 July 2019
Original Article

ORIGINAL ARTICLE

Early Forebrain Neurons and Scaffold Fibers in Human Embryos

Jingwen Qin[1,†], Meizhi Wang[1,†], Tianyun Zhao[2,†], Xue Xiao[1], Xuejun Li[1], Jieping Yang[3], Lisha Yi[3], Andre M. Goffinet[1], Yibo Qu[1,4] and Libing Zhou[1,4,5]

[1]Guangdong-Hongkong-Macau Institute of CNS Regeneration, Ministry of Education CNS Regeneration Collaborative Joint Laboratory Jinan University Guangzhou 510632, P.R. China [2]Department of Anesthesiology, Guangzhou Women and Children's Medical Center Guangzhou Medical University Guangzhou, P.R. China [3]Department of Obstetrics and Gynecology, Guangzhou Women and Children's Medical Center Guangzhou Medical University Guangzhou, P.R. China [4]Guangzhou Regenerative Medicine and Health Guangdong Laboratory Guangzhou 510530, P.R. China, and [5]Key Laboratory of Neuroscience, School of Basic Medical Sciences; Institute of Neuroscience, The Second Affiliated Hospital Guangzhou Medical University Guangzhou 511436, P.R. China

Address correspondence to Libing Zhou and Yibo Qu, Guangdong-Hongkong-Macau Institute of CNS Regeneration, Jinan University, Huangpu Avenue West601, Guangzhou 510632, P.R. China. Email: tlibingzh@jnu.edu.cn (L. Zhou) and tquyibo@jnu.edu.cn (Y. Qu)
[†]Those authors contributed equally to this work

Abstract

Neural progenitor proliferation, neuronal migration, areal organization, and pioneer axon wiring are critical events during early forebrain development, yet remain incompletely understood, especially in human. Here, we studied forebrain development in human embryos aged 5 to 8 postconceptional weeks (WPC5–8), stages that correspond to the neuroepithelium/early marginal zone (WPC5), telencephalic preplate (WPC6 & 7), and incipient cortical plate (WPC8). We show that early telencephalic neurons are formed at the neuroepithelial stage; the most precocious ones originate from local telencephalic neuroepithelium and possibly from the olfactory placode. At the preplate stage, forebrain organization is quite similar in human and mouse in terms of areal organization and of differentiation of Cajal-Retzius cells, pioneer neurons, and axons. Like in mice, axons from pioneer neurons in prethalamus, ventral telencephalon, and cortical preplate cross the diencephalon–telencephalon junction and the pallial–subpallial boundary, forming scaffolds that could guide thalamic and cortical axons at later stages. In accord with this model, at the early cortical plate stage, corticofugal axons run in ventral telencephalon in close contact with scaffold neurons, which express CELSR3 and FZD3, two molecules that regulates formation of similar scaffolds in mice.

Key words: axonal projection, human embryos, pioneer fibers, predecessor neurons, preplate

Introduction

Unraveling the intricate cellular and molecular mechanisms that direct human forebrain development is crucial to understanding cognitive processes in normal and pathological conditions. Our present view about these complex issues is mostly based on studies of rodents and, to a lesser extent, carnivores and monkeys (Parnavelas 2000; Smart et al. 2002; Reillo and Borrell 2012; Florio and Huttner 2014). Until recently, human data were scarce, conserved in collections and illustrated in atlases (Bayer and Altman 2002; O'Rahilly and Müller 2006). Interest in human neural development was recently rekindled

(Clowry et al. 2010), in parallel to the availability of novel molecular and cellular methods such as RNA sequencing (Florio et al. 2017) or induced neural stem cells and organoid cultures (Suzuki and Vanderhaeghen 2015; Di Lullo and Kriegstein 2017; Pasca 2018). With some notable exceptions (Larroche 1981; Marin-Padilla 1983; Zecevic et al. 1999; Meyer et al. 2000; Meyer et al. 2002; Bystron et al. 2005; Bystron et al. 2006; Casoni et al. 2016; Clowry et al. 2018), most studies of human focused on fetal developmental stages, later than 8–10 weeks postconception (WPC), rather than on embryonic development (up to WPC8). Yet, work in rodents, carnivores, and non-human primates (Allendoerfer and Shatz 1994; Molnar and Clowry 2012; Dehay et al. 2015) points to the importance of early developmental events, not only to pattern the areal organization of the forebrain (O'Leary and Sahara 2008; Hoch et al. 2009; Rakic et al. 2009) but also for setting an early wiring blueprint (Molnar and Clowry 2012; Hua et al. 2014; Qu et al. 2014; Alzu'bi et al. 2019). Data in animal models therefore emphasize the need to study further early human embryonic brain development in the light of modern developmental concepts (Clowry et al. 2010), as addressed in some recent publications (Bystron et al. 2005; Casoni et al. 2016; Alzu'bi et al. 2017b; Clowry et al. 2018).

The present study is focused on the embryonic period, from WPC5 to WPC8. At the neuroepithelial stage (WPC5), radial progenitors in the ventricular zones divide symmetrically to increase the progenitor pool (Florio and Huttner 2014); they also may generate early neurons by asymmetric division leading to direct neurogenesis. This is followed by the preplate (PP) stage at WPC6–7, when a loose network of horizontal neurons appears in the dorsal telencephalon and some pioneer axons form in ventral telencephalic regions (Meyer et al. 2000; Clowry et al. 2010). At that stage, cortical neurogenesis occurs through formation of TBR2-positive intermediate progenitors that divide a few times to form neurons (Vasistha et al. 2015). REELIN (RELN)-positive cells, especially Cajal-Retzius cells, are generated around the cortical primordium and migrate tangentially in subpial position (Meyer et al. 2000; Bielle et al. 2005; Pedraza et al. 2014); they are different from PP pioneer neurons. At WPC8, the incipient cortical plate (CP) appears. It is formed by radial migration of glutamatergic neurons derived from radial progenitors and intermediate progenitors in ventricular and, later, subventricular zones, which are especially large in human in comparison with rodents (Smart et al. 2002). Radial migration leads to formation of the different cortical layers in an inside-to-outside pattern, with sequential formation of deep (6 and 5) and upper (4, 3, and 2) cortical layers. CP neurons send axonal projections that travel through the ventral telencephalon towards the dorsal thalamus. In parallel, axons from dorsal thalamus run through the prethalamus and the ventral telencephalon, en route to the cortical primordium (Molnar, et al. 1998b; Molnar and Cordery 1999; Molnar and Clowry 2012). In addition, cortical GABAergic interneurons generated in ventricular zones in ventral telencephalon reach the cortex by tangential migration (Marin 2013). We choose not to address stages later than WPC8, concerned with the formation and maturation of the CP, which are described and discussed elsewhere (Bayatti et al. 2008; Al-Jaberi et al. 2015; Alzu'bi, et al. 2017a).

Our observations confirm the appearance of precocious forebrain neurons and neurites at WPC5. Some appeared to be generated locally in the telencephalic neuroepithelium. Another contingent seemed to originate from the olfactory placode (OLP) and to migrate tangentially in the hypothalamic and preoptic anlage zone. In the OLP, most cells were positive for TUJ1, Calretinin and Doublecortin (DCX), and expressed GnRH mRNA later at the PP stage (Schwanzel-Fukuda et al. 1992; Casoni et al. 2016). Precocious neurons were reminiscent of and possibly similar to predecessor neurons (Meyer et al. 2002; Bystron et al. 2005; Bystron et al. 2006). At PP stages, WPC6–7, developmental sequences followed the pattern described in other mammals. RELN-positive Cajal-Retzius cells were abundant in the region of the anti-hem and spread in the subpial marginal zone, prior to their origin in the hem, which was better defined later, from WPC8. Loose tangential neuronal nets developed in the telencephalic PP and diencephalon, prior to the appearance of CP, striatal and dorsal thalamic neurons. In the dorsal telencephalon, the PP neuronal population contributed early fibers across the pallial–subpallial boundary (PSPB). At the same time, fibers from early neurons in the ventral telencephalon and prethalamus crossed the diencephalon–telencephalon junction (DTJ) in both directions, forming a scaffold as described in mice (Feng et al. 2016). A large proportion of early ventral telencephalic scaffold cells expressed ISL1. At WPC8, axons from early CP cells crossed the PSPB and ran in close contact with ISL1-positive cells, suggesting that the latter acted as guideposts. In situ hybridization showed that CELSR3 and FZD3, two molecules that control the formation of the guidepost scaffold in mice (Tissir and Goffinet 2013; Qu et al. 2014; Feng et al. 2016), were expressed strongly in the dorsal, ventral telencephalon and prethalamus.

Table 1. Number of embryos

Age	ISH	Immunostaining and histology	DiI implantation	Total
WPC5	1	7	0	8
WPC6	2	4	2 (in the Ncx)	8
WPC7	2	5	5 (3 in the vTel and 2 in the pTh)	12
WPC8	2	3	3 (2 in the Ncx and 1 in the vTel)	8

ISH, in situ hybridization; Ncx, Neocortex; vTel, ventral telencephalon; pTh, prethalamus.

Materials and Methods

Human Tissue

Human samples were obtained following drug-induced abortions at Guangzhou Women and Children's Medical Center. All procedures were approved by the Medical Ethics Committees of the hospital (ref file 2016041303) and of Jinan University and are in accordance with the Helsinki convention. Informed consent was obtained from both parents, and pregnant women had no reported disease history. After expulsion, embryos without apparent macroscopic malformation were fixed in 4% paraformaldehyde (PFA) in 0.01M phosphate buffered saline (PBS) or in Bouin's fixative at 4°C. Embryonic age was estimated by the date of the mother's last menstruation and by measurements of Crown Rump length referring to a growth chart (Hern 1984). Embryos were also staged as described (Bayer and Altman 2002; O'Rahilly and Müller 2006), using the online atlas available at www.visembryo.com. Embryonic specimens are listed in Table 1.

Table 2. Primary antibodies

Antibody	Source	Dilution	Cat. No.	Company	Method
ISL1	Mouse	1:1000	ab26122	Abcam	IHC
TBR1	Rabbit	1:500	ab31940	Abcam	IHC/IF
TBR2	Rabbit	1:5000	ab2283	Millipore	IHC
Reelin	Mouse	1:1000	142	A. Goffinet	IHC/IF
Reelin	Mouse	1:2000	G10	A. Goffinet	IHC
MASH1	Rabbit	1:6000	ab74065	Abcam	IHC
PAX6	Mouse	1:500	ab78545	Abcam	IHC
NF-160	Mouse	1:500	n5264	Sigma	IHC/IF
ISL1	Mouse	1:800	ab20670	Abcam	IF
TBR2	Goat	1:500	sc-69 269	Santa Cruz	IF
TBR1	Mouse	1:500	ab18302	Abcam	IF
TUJ1	Rabbit	1:3000	2128	Cell Signaling Tech.	IF
TUJ1	Mouse	1:4000	T8660	Abcam	IF
DCX	Goat	1:500	sc-8066	Santa Cruz	IF
GAD65	Mouse	1:1000	ab26113	Abcam	IF
PAX6	Rabbit	1:500	ab195045	Abcam	IF
PH3	Mouse	1:200	ab14955	Abcam	IF
Calbindin	Rabbit	1:1000	ab108404	Abcam	IF
Calretinin	Rabbit	1:100	ab702	Abcam	IF
Ki67	Rabbit	1:500	ab15580	Abcam	IF
CTIP2	Rat	1:500	ab18465	Abcam	IF
P75NTR	Mouse	1:600	ab8874	Abcam	IF

IHC, immunohistochemistry; IF, Immunofluorescence.

Histology and Immunohistochemistry

After 24-hour fixation, the skin was removed under a dissection microscope to expose the brain. Bouin-fixed brains were embedded in paraffin and sectioned at 8-µm thickness for hematoxylin eosin (HE) staining and immunohistochemistry. PFA-fixed brains were cryoprotected in sucrose-PBS, prior to preparation of 10-µm-thick cryostat sections for immunofluorescence. Paraffin sections were deparaffinized and progressively rehydrated to 0.01 M PBS prior to antigen retrieval in 10-mM citric acid (pH 6.0) at 60°C for 30 min. Frozen sections were rinsed in 0.01M PBS prior to antigen retrieval. After blocking (10% normal donkey serum, 0.1% Triton X-100 in PBS) for 30 min at room temperature, sections were incubated with primary antibodies (Table 2) overnight at 4°C. Signal was detected using an ABC kit (PK-6200, Universal, Vector) for paraffin sections, or with secondary antibodies labeled with Alexa Fluor 405, 488, 546, 594, or 647 (all from Invitrogen, 1:1000). The signal of anti-MASH1 was disclosed using a VIP kit (blue; Cat. No. SK-4600, Burlingame, CA USA).

DiI Tracing

PFA-fixed brains were embedded in 4% low-melting-point agarose (Cat. No. 111860, Biowest, Spain) and 800-µm vibratome sections were prepared. Under a dissection microscope, small DiI crystals (D3911, Molecular Probes) were placed in ventral telencephalon, ventral thalamus, dorsal thalamus, or cortex. After incubation for 2 weeks at 37°C in 0.01M PBS containing 0.08% NaN_3, samples were sectioned at 100-µm thickness using a vibratome and observed by fluorescence microscopy.

mRNA In Situ Hybridization

Samples were prepared under RNAse-free conditions, and in situ hybridization (ISH) was carried out using probes for human CELSR3 (Cat. No.322350), FZD3 (Cat. No. 310091) and GnRH (Cat. No. 562591), mouse Celsr3 (Cat. No. 319241) and Fzd3 (Cat. No. 404891) designed by Advanced Cell Diagnostic, according to the protocol and with reagents provided in the RNAscope® kit (Advanced Cell Diagnostics, Inc.). Briefly, PFA-fixed 10-µm frozen coronal sections were washed in 0.01M PBS for 5 min and sequentially treated with RNAscope® Hydrogen Peroxide for 10 min at room temperature, RNAscope® Target Retrieval for 30 min at 99–100 °C, and RNAscope® Protease Plus for 30 min at 40°C. Hybridization with or without (negative control) probe was performed for 2 h at 40°C in the HybEZ™ Humidity Control Tray (Advanced Cell Diagnostics, Inc.; Cat. No.310012), and the signal was disclosed by incubation in the "RED" working solution for 10 min at room temperature. Images were captured with a confocal microscope (Zeiss LSM 700, Germany) or a fluorescent microscope (Zeiss Imager A2, Germany).

Results

As mentioned in the Introduction, we focus on three embryonic stages, namely, 1) the neuroepithelial and early marginal zone (NE) stage when cerebral hemispheres begin to bulge just after neural tube closure, which corresponds to WCP5 or to Carnegie stages (CS) 15 and 16; 2) the stage when the early PP network of horizontal neurons and pioneer fibers appear in the forebrain, at WPC6 and 7 (CS17–19); and 3) the stage when the incipient cortical plate (CP) emerges at WPC8 (CS20–22). We lay specific emphasis on the description of early neurons at the NE stage and on components of a guidepost scaffold between diencephalon and telencephalon at the PP and early CP stages.

Early Telencephalic Neurons at the NE Stage

During early forebrain neurogenesis, radial progenitors proliferate along ventricles by symmetric division, before undergoing asymmetric divisions and generating early neurons directly or,

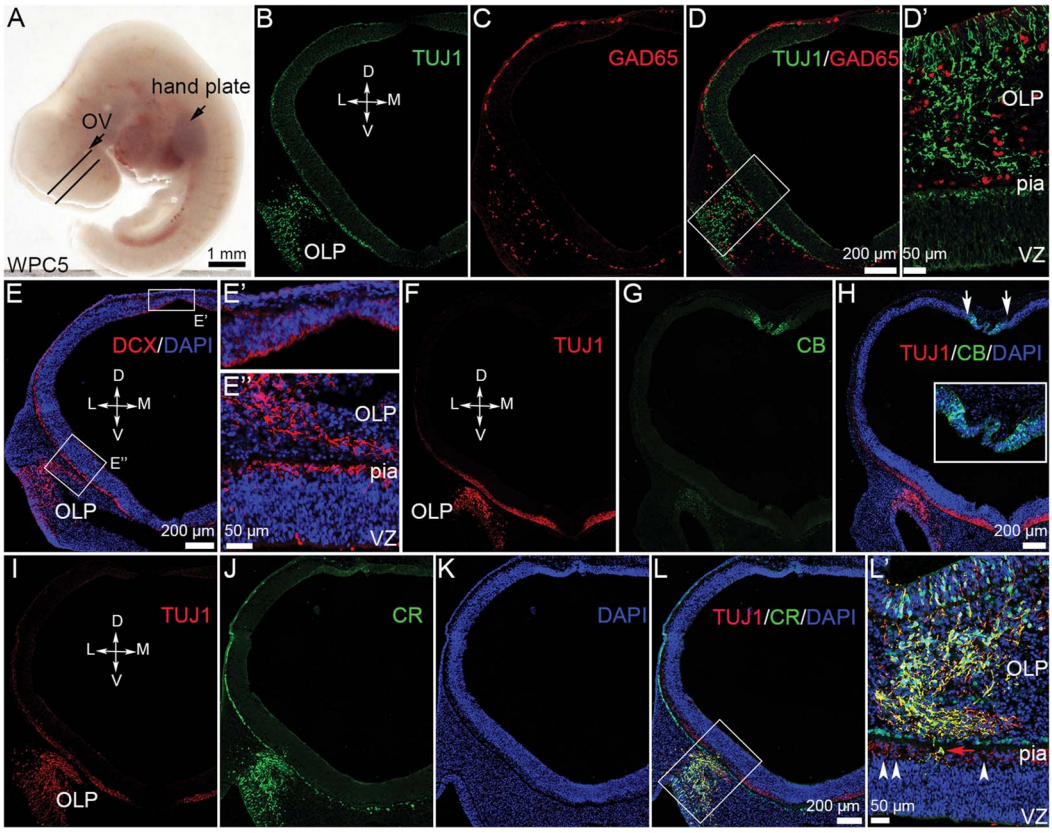

Figure 1. **Precocious neurons at the neuroepithelial stage**. *A*: Lateral view of a WPC5 embryo, showing the optic vesicle (OV) and the hand plate, but no evidence of foot plate. Lines indicate the orientation of sections. *B–D′*: TUJ1 (green, *B*) and GAD65 (red, *C*) double immunostaining. Strongly labeled TUJ1-positive cells are present in a subpial position and in the olfactory placode (OLP) (*B*), and there is no specific GAD65 signal in neural tissue (*C*) and no colocalization of TUJ1 and GAD65 (*D*). At higher magnification, TUJ1-positive cells are visible in the OLP and the superficial regions of telencephalic wall and only non-specific GAD65 signal is seen in the OLP (*D′*, selected area in *D*). *E–E″*: DCX immunoreactivity is detected in progenitors in the ventricular zone of the most medial–dorsal region of the telencephalon and in migrating cells in the OLP and the external region of telencephalic wall (*E′* and *E″*, selected areas in *E*). *F–H*: TUJ1 (red, *F*) and Calbindin (CB, green, *G*) double immunofluorescent staining in the prosencephalon. CB-positive signal is only identified in the most dorsal region of the telencephalic wall (*G*), which is negative for TUJ1 (*H*, the enlarged inset from arrow-indicated region). DAPI counterstains nuclei (blue). *I–L′*: TUJ1 (red, *I*) and Calretinin (CR, green, *J*) double immunofluorescent staining. CR-positive cells are enriched in the OLP (*J*) and entirely overlap with TUJ1-posive cells (*L*, *L′*). The high magnification shows a CR and TUJ1 double positive cell possibly migrating from the OLP towards the telencephalic wall (red arrow in *L′*); TUJ1-positive cells below the pia are negative for CR (arrowheads in *L′*). *L′*, selected area in *L*. DAPI counterstains nuclei (blue, *K*). The compass indicates anatomical orientation (*B*, *E*, *F*, *I*): D, dorsal; V, ventral; M, medial; L, lateral.

later, via generation of intermediate progenitor cells that divide symmetrically into neurons (Englund et al. 2005; Arnold et al. 2008; LaMonica et al. 2012; Florio and Huttner 2014; Vasistha et al. 2015; Ostrem et al. 2017).

At the NE stage (Fig. 1A), the prospective cerebral hemispheres were not clearly separated and surrounded a "telencephalic superventricle" (Bayer and Altman 2002) (Fig. 1B–L). To identify early telencephalic neurons, we first carried out anti-neuronal beta 3 tubulin (TUBB3, aka TUJ1) immunofluorescence and found that some positive, presumably neuronal cells were widely scattered in the telencephalic wall below the pia and were also abundant in the OLP (Fig. 1B). The distinctive neuronal morphology of TUJ1-positive cells was evidenced by their rounded or spindle-shaped soma associated with short neurites occasionally capped with growth cones (Fig. 1D′). A stream of TUJ1-positive cells appeared to join the OLP and the telencephalic wall (Fig. 1B). Immunofluorescent staining for GAD65, a marker of some early neurons (Garcia-Pena et al. 2014) did not disclose any neuron-like cells and showed only signal associated with meningeal cells and probably some blood cells in the OLP (Fig. 1C); no TUJ1 and GAD65 double-labeled cells were seen (Fig. 1D,D′). To try and confirm the origin of those precocious neurons, we used anti-DCX immunofluorescence to label migrating cells and observed a distribution similar to that of TUJ1-positive cells (Fig. 1E,E″). In addition, some DCX staining cells were seen in the dorsal–medial region of the cortical wall (Fig. 1E,E″), probably associated with dorsal radial progenitors as described in rodents (Walker et al. 2007). Abundant Calbindin-positive, TUJ1 negative cells were also visible in that DCX-positive region (Fig. 1F–H), which might correspond to the future cortical hem (Gonzalez-Gomez and Meyer 2014). In the OLP, double immunofluorescent staining showed that all TUJ1-positive cells co-expressed Calretinin (Fig. 1I–L′) and that some double-labeled cells extended across the boundary between the OLP and telencephalic wall (red arrow in Fig. 1L′). However, most TUJ1-positive telencephalic cells were negative for Calretinin at this stage (white arrowheads in Fig. 1L′). No specific CTIP2-positive or P75NTR-positive cells were seen in the telencephalic wall or the OLP (Supplementary Figure 1).

To assess further the origin of early TUJ1-positive cortical neurons, we studied progenitor cells using combined immunofluorescence for PAX6, a marker of radial dorsal

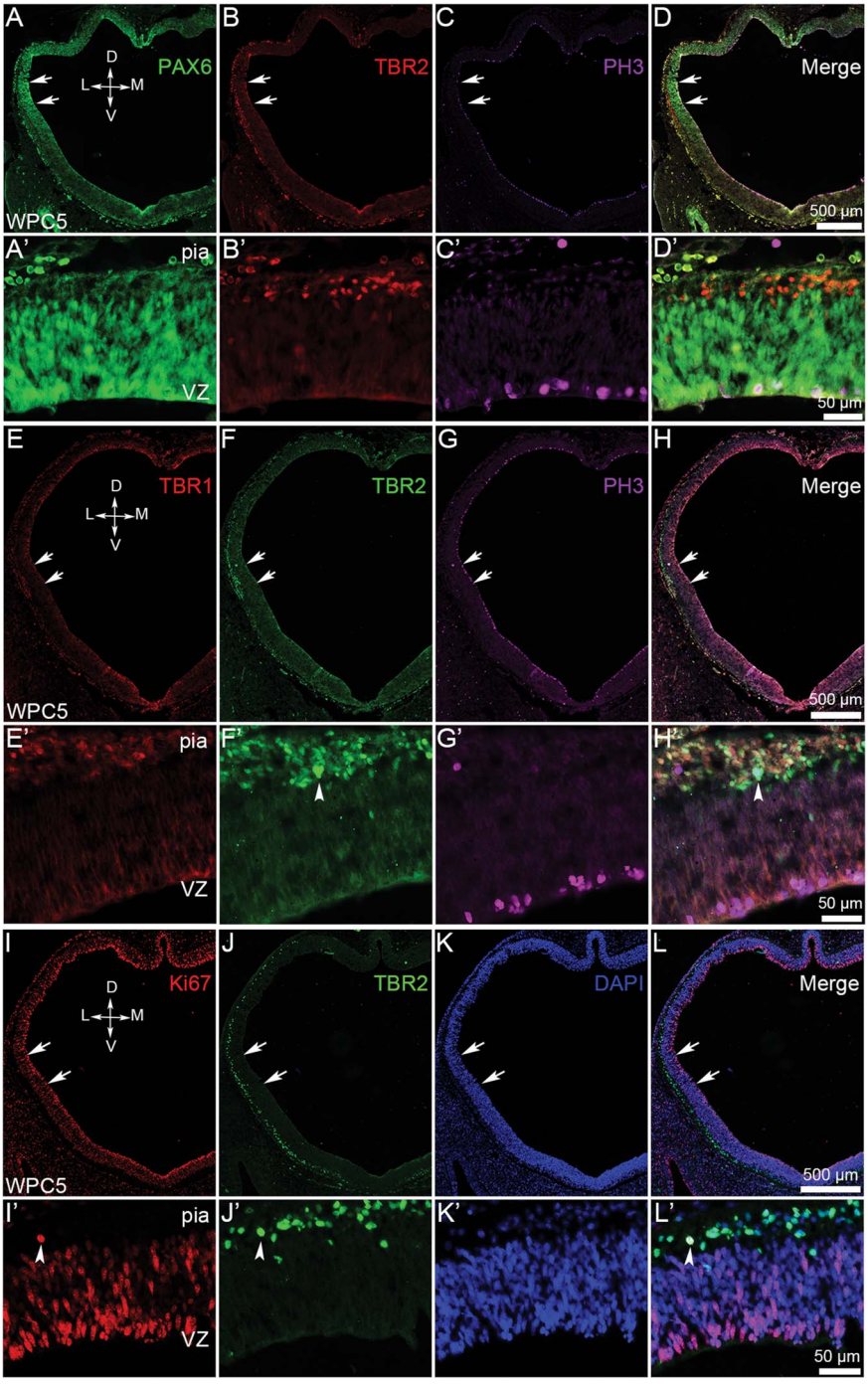

Figure 2. **Neural progenitors in the human prosencephalon at the neuroepithelial stage.** *A–D′*: PAX6 (green, *A* and *A′*), TBR2 (red, *B* and *B′*) and PH3 (purple, *C* and *C′*) triple immunofluorescent staining inWPC5 forebrain sections. PAX6-signal is restricted in the dorsal region of the telencephalic wall, mostly in the ventricular zone (*A′*). In the merged image (*D*, *D′*), all PH3-positive cells co-express PAX6, but TBR2-positive cells are negative for PAX6. *A′–D′* correspond to areas indicated by arrows in *A–D*. *E–E′*: TBR1 (red, *E* and *E′*), TBR2 (green, *F* and *F′*) and PH3 (purple, *G* and *G′*) triple immunofluorescent staining inWPC5 forebrain sections. TBR1-stained nuclei are scattered in the subpial location of the telencephalic wall laterally (*E*, *E′*), and there is some fiber-like TBR1-positive signal in the ventricular zone (probably non-specific staining; *E′*). TBR2-positive cells are distributed below the pial surface in the lateral region of the telencephalic wall (*F*, *F′*). PH3-positive cells are aligned in the entire ventricular zone (*G*, *G′*). In the merged image (*H*), no TBR1 or TBR2 positive cells express PH3; most TBR1-positive cells co-express TBR2 and a few TBR2-positve cells are negative for TBR1 (*H′*). One example of TBR2-positive and TBR1-negative cells is indicated by arrowheads in *F′* and *H′*. *E′–H′* correspond to areas indicated by arrows in *E–H*. *I–L′*: Ki67 (red, *I* and *I′*) and TBR2 (green, *J* and *J′*) double immunofluorescent staining in WPC5 forebrain sections. Abundant Ki67-positive cells are distributed in the entire telencephalic wall, more in the ventricular zone (*I*, *I′*). In the merged image (*L*, *L′*), a few TBR2-positive cells are also Ki67-positive (one example indicated by arrows in *I′*, *J′*, and *L′*). DAPI counterstains nuclei (*K*, *K′*). *I′–L′* correspond to areas indicated by arrows in *I–L*. The compass shows the orientation of sections (*A*, *E*, *I*): D, dorsal; V, ventral; M, medial; L, lateral.

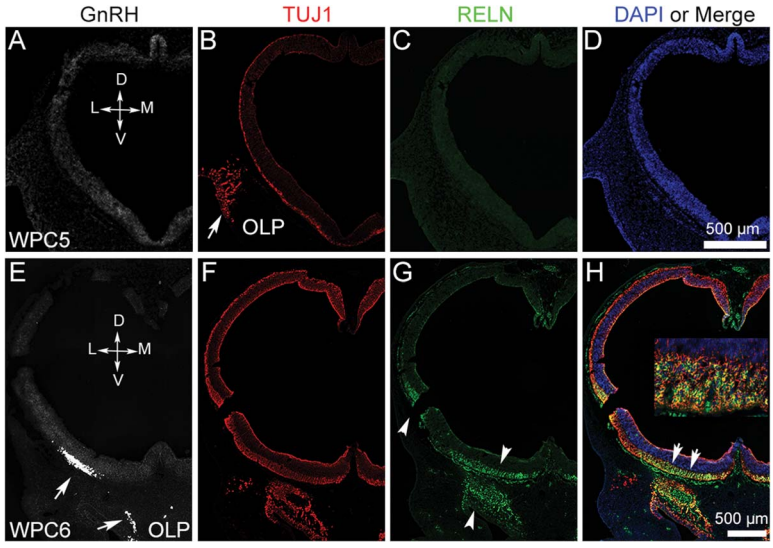

Figure 3. **GnRH and RELN expression in precocious neurons.** *A–D*: At WPC5, there is no GnRH-positive signal in the telencephalic wall or the olfactory placode (OLP) using ISH (*A*). In an adjacent section, some TUJ1-positive precocious neurons are visualized in the OLP (arrow) and the cortical wall (*B*), but no RELN-positive cells are found in these regions (*C*). DAPI stains nuclei (*D*). *E–H*: At WPC6, GnRH mRNA is present in the ventral compartment of the telencephalic wall and the OLP (*E*, indicated by arrows), where TUJ1-positive cells are abundant (*F*) and some RELN-positive cells are seen (*G*, indicated by arrowheads). Merged picture shows RELN-positive cells that are also positive for TUJ1 (*H*). The inset corresponds to the enlarged area indicated by arrows in *H*. The compass indicates anatomical orientation (*A*, *E*): D, dorsal; V, ventral; M, medial; L, lateral.

telencephalic progenitors, for the immature neuronal markers TBR1 and TBR2, the mitotic cell marker phosphohistone 3 (PH3), and the progenitor proliferation marker Ki67 (Fig. 2). At WPC5, PAX6 expression was confined to the VZ as predicted. High expression was found in the lateral region of the telencephalic wall, with a well-defined lateral–ventral border that presumably marked the future frontier between dorsal and ventral telencephalon and a decreasing lateral to medial gradient (Fig. 2A,A′; Supplementary Figure 2). Using the immature cortical neuron marker TBR1 (Englund et al. 2005), we found TBR1-positive cells in the external tier of the telencephalic wall, in the lateral region with high PAX6 expression; in addition, some, presumably nonspecific signal was associated with the ventricular zone (Fig. 2E,E′). TBR2-positive cells had a distribution quite similar to that of TBR1 below the pial surface in the lateral field corresponding to high PAX6 expression, but no expression was detected in VZ (Fig. 2B,B′,F,F′). PH3-positive cells were scattered in the entire ventricular zones (Fig. 2C,C′,G,G′). In PAX6-positive sectors, all PH3-positive cells co-expressed PAX6 (Fig. 2A′,C′,D′), whereas no TBR1- or TBR2-positive cells expressed PH3 (Fig. 2H,H′). In addition, few if any TBR2-posositive cells expressed PAX6 (Fig. 2D′). Most (about 95%) TBR1-positive cells were positive for TBR2, whereas about 30% of TBR2-positive cells were negative for TBR1 (Fig. 2E′,F′,H′). The expression patterns of PAX6, TBR2, and PH3 were similar at rostral and caudal levels (Supplementary Figure 2). As PH3 labels a small subset of dividing cells (Fig. 2C,G), we also performed double immunostaining for TBR2 and Ki67 to assess whether some TBR2-positive cells were engaged in cell division. Abundant Ki67-positive cells were distributed in the entire telencephalic wall (Fig. 2I,I′). Only about 4% of TBR2-positive cells co-expressed Ki67 (Fig. 2I–L,I′–L′).

It was reported that some GnRH-positive precocious neurons migrate from the OLP to the neural tube (Casoni et al. 2016). To assess whether these early TUJ1-positive neurons also express GnRH or RELN, we performed GnRH RNAscope ISH and double immunostaining for TUJ1 and RELN in adjacent sections. At WPC5, we did not see any GnRH-positive or RELN-positive signal associated with early TUJ1-positive cells in the telencephalic wall or the OLP (Fig. 3A–D). At WPC6, GnRH mRNA was visualized in the ventral compartment of the forebrain and the OLP (Fig. 3E), two regions where TUJ1-positive cells were abundant (Fig. 3F). At this stage, numerous RELN-positive cells were detected in the ventral hemisphere and some were seen in the OLP (Fig. 3G), and they were positive for TUJ1 (Fig. 3H).

Similar Overall PP Organization in Human and Mouse

The PP is a loose horizontal and transient network of early cortical neurons, where critical events control subsequent cortical development (Meyer 2001; Wang et al. 2010). In the mouse, the PP forms around embryonic day (E) 12.5 (Super et al. 1998) and in human embryos at WPC6–7 (Meyer 2001).

At PP stages, the forebrain was clearly divided into telencephalon and diencephalon (Fig. 4A,B). In HE-stained sections, different sectors were defined, including the dorsal telencephalon with its incipient medial, dorsal, and lateral cortical divisions, the ventral telencephalon, the dorsal thalamus, the prethalamus, and the hypothalamus (Fig. 4C,D), an overall organization quite similar to that of the E12.5 mouse forebrain (Fig. 4E,F). Heavily packed radial progenitor cells were aligned in ventricular zones along the lateral ventricles, in the medial and lateral ganglionic eminences (MGE and LGE) at the rostral level (Fig. 4C) and more caudally in the caudal ganglionic eminence (CGE) and along the third ventricle (Fig. 4D). Cells with a tangential orientation, presumably neurons, were scattered in the subpial region (Fig. 4G). DiI implantation in WPC7 cortices resulted in labeling of pioneer PP neurons and prominent horizontal neurites (Fig. 4H) (Super et al. 1998; Zecevic et al. 1999).

In mice, Pax6 and Mash1 (aka Ascl1) are key regulators of neurogenesis in dorsal and ventral telencephalon, respectively

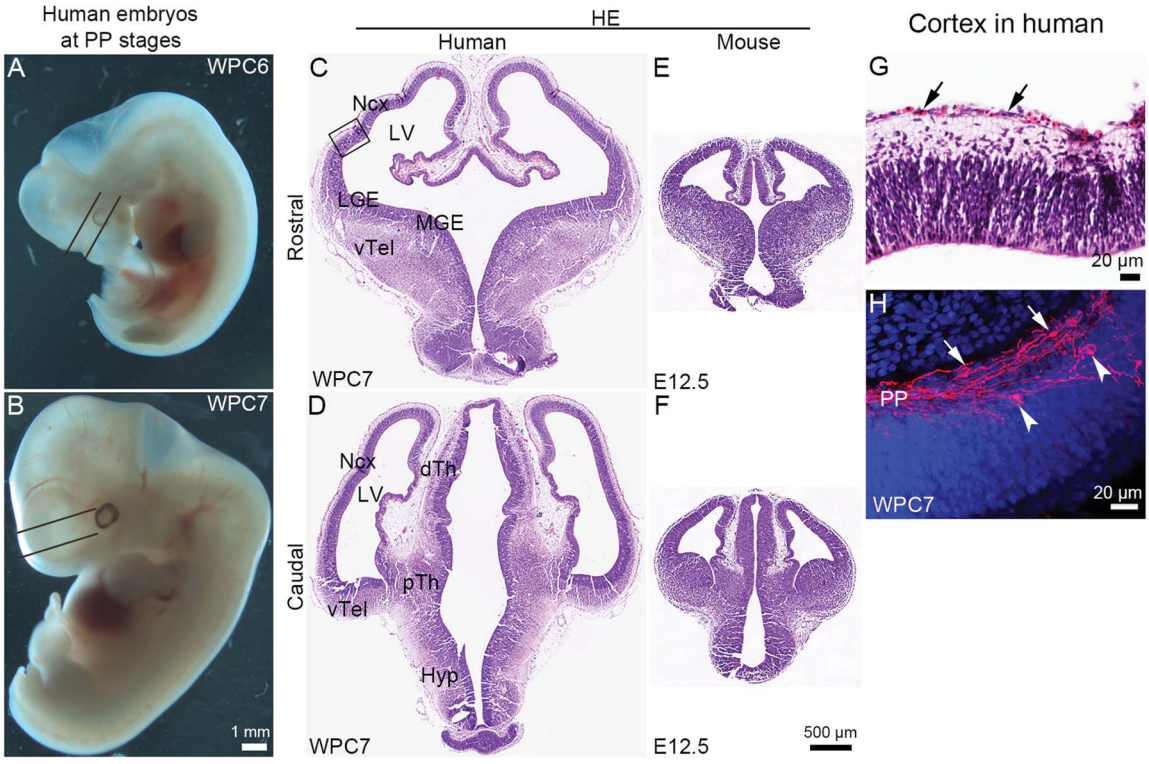

Figure 4. **Overall organization at the PP stage**. *A*, *B*: Lateral views of human embryos at WPC6 (*A*) and WPC7 (*B*). Lines indicate section orientation. *C*–*G*: HE staining of WPC7 human (*C*, *D*) and E12.5 mouse (*E*, *F*) sections shows the similar architectonic organization in both species. High magnification shows progenitor cells in the ventricular zone and tangentially aligned cells in the PP (*G*, arrows). MGE, medial ganglionic eminence; LGE, lateral ganglionic eminence. *H*: DiI implantation into the cortex labels a few pioneer cells in the superficial region (arrows) and profuse fibers in the plexiform primordial layer (arrowheads). PP: preplate.

(Casarosa et al. 1999; Toresson et al. 2000). We compared the expression of these transcription factors in WPC7 human and E12.5 mouse embryos. In both species, PAX6 expression was confined to the ventricular zone of the dorsal telencephalon, with a lateral–medial decreasing gradient that was already noticed at WPC5. The PAX6 expression domain extended slightly ventral to the angle of the lateral ventricle (Fernandez et al. 1998), in progenitors of the future claustrum–amygdala complex (Butler and Hodos 2005; Puelles 2017) (Fig. 5*A*,*E*, arrow). At caudal levels, PAX6 was also heavily expressed in the ventricular zone in the diencephalon and expression extended to postmitotic neurons in the prethalamus (Fig. 5*B*,*F*). This expression profile was comparable with that in E12.5 mouse forebrain (Fig. 5*C*,*D*). MASH1 was expressed in a pattern largely complementary to that of PAX6, with high level in ganglionic eminences (LGE and MGE) (Fig. 5*E*,*F*), which was similar to that in mouse forebrain (Fig. 5*G*,*H*). This complementarity was confirmed by double PAX6 and MASH1 immunostaining, which showed very little if any overlap (Fig. 5*E*,*F*).

In WPC7 human forebrain, young TBR1-positive neurons were widely scattered beneath the pia in the entire telencephalon from rostral to caudal levels, up to the PSPB; they were also abundant in the prethalamus (Fig. 5*I*,*J*; see also Fig. 8*A*), a distribution that was comparable with that in mice (Fig. 5*K*,*L*). At that stage, the TBR2-positive signal was associated with cells in the subventricular zone, between ventricular zones and the layer of early PP neurons, up to the level of the PSPB (Fig. 5*M*,*N*; see also Fig. 8*A*), which was comparable with mouse (Fig. 5*O*,*P*). In the PP, contrary to the NE stage, there was only some minor colocalization of TBR1 and TBR2 expression (Fig. 8*A*1^{iv}).

Early RELN-positive Neurons in Human Forebrain

Given the key role of RELN during cortical development (Meyer et al. 2000; Tissir and Goffinet 2003), we studied RELN-positive cells using immunofluorescence (de Bergeyck et al. 1998). Strong signal was associated with horizontal subpial Cajal-Retzius cells distributed all over the cortical primordium at WPC7 (Fig. 6*A*), but RELN was not detected in PP neurons located deeper in the marginal zone (Fig. 6*A*′–*A*‴). In addition, moderately RELN-positive neurons were abundant in some diencephalic structures, presumably components of future reticular thalamus and zona incerta (data not shown) (Schiffmann et al. 1997). Positive cells were also seen in the ventral telencephalon, possibly corresponding to early interneurons (Fig. 6*A*). At those early stages, very few if any RELN-positive cells were found in the cortical hem (Fig. 6*A*), and most seemed to originate in the area of the anti-hem or the region where DBX1-positive progenitors are described in ventral pallial and septal areas (Bielle et al. 2005). At WPC8, abundant RELN-positive cells were found in the ventral telencephalon and the cortical marginal zones, as well as in the cortical hem (Fig. 6*B*,*B*′–*B*‴).

A Guidepost Scaffold in the Forebrain at the PP and Early CP Stages

In rodents, developing thalamocortical and corticothalamic tracts need to cross the PSPB and the DTJ, and this begins at the incipient CP stage (Metin and Godement 1996; Molnar et al. 1998a; Molnar and Cordery 1999; Garel and Lopez-Bendito 2014). Our previous work showed that two populations of ISL1-

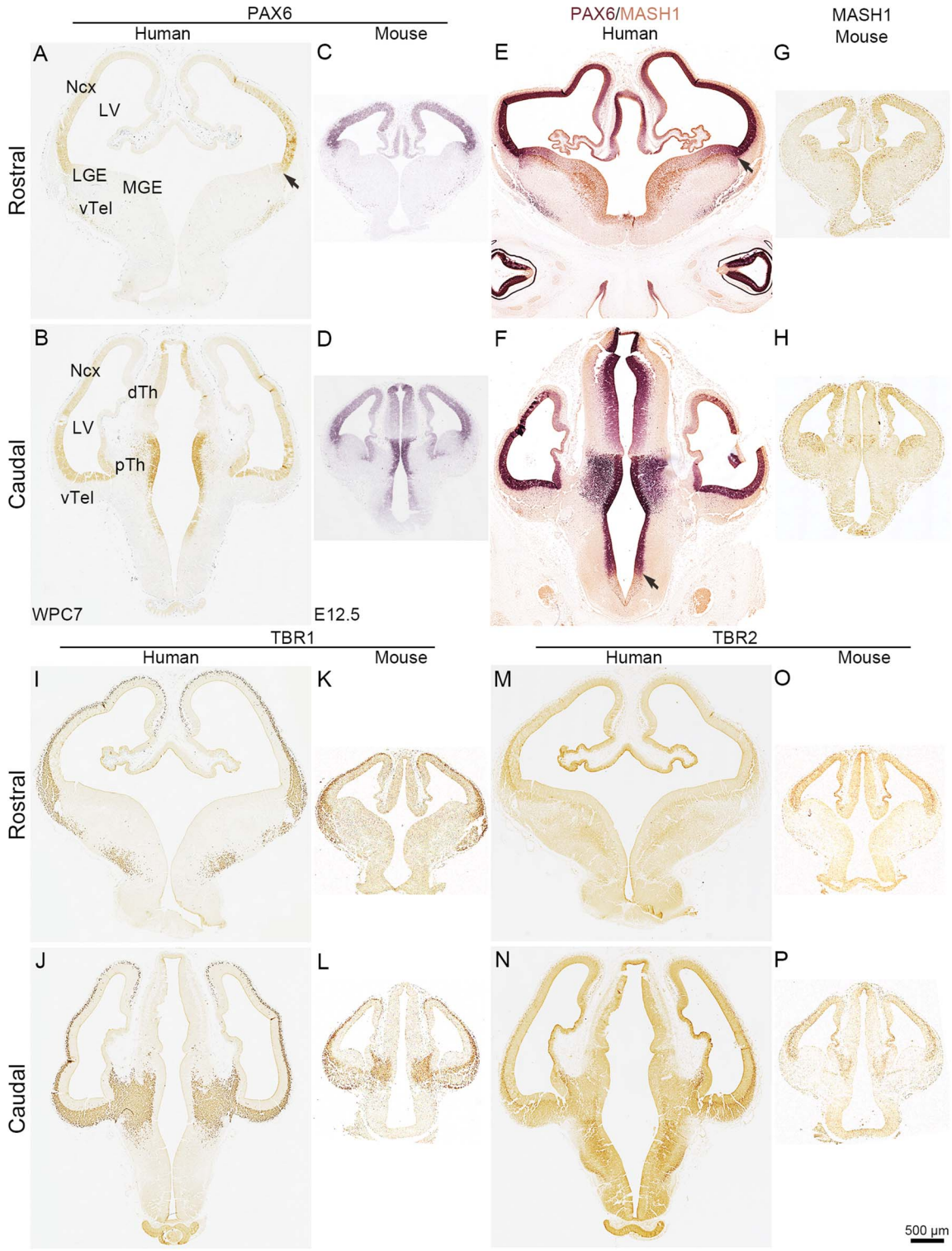

Figure 5. **Areal organization and early neurogenesis at the PP stage.** *A–D*: PAX6 immunostaining in WPC7 human (*A*, *B*) and E12.5 mouse forebrain (*C*, *D*). In both species, PAX6-positive signal is confined to the ventricular zone of the cortex (Ncx), with a focal extension ventral to the angle of the lateral ventricle (arrow in *A*), close to the lateral ganglionic eminence (LGE). PAX6 is also expressed in diencephalic ventricular zones and in prethalamus (pTh) (*B*). LV: lateral ventricle; MGE: medial ganglionic eminence; vTel: ventral telencephalon; dTh: dorsal thalamus. *E–H*: MASH1 immunostaining in human (*E*, *F*, MASH1, brown, combined with PAX6 in purple) and mouse forebrain (*G*, *H*). Arrows in *E* and *F* indicate the border between MASH1 and PAX6 expression domains. *I–L*: TBR1 immunostaining in human (*I*, *J*) and mouse (*K*, *L*) shows similar expression patterns. *M–P*: TBR2 immunostaining in human (*M*, *N*) and mouse (*O*, *P*) forebrain reveals a similar distribution of intermediate progenitor cells.

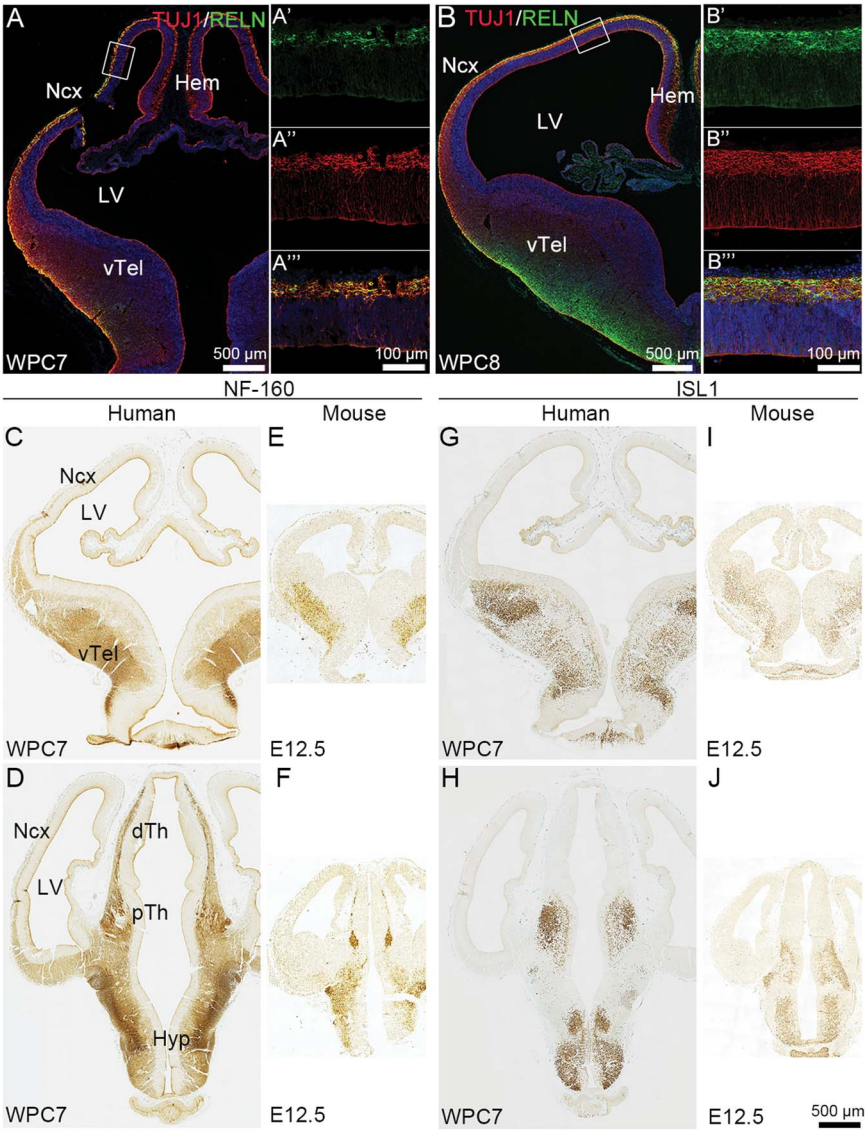

Figure 6. **Early fibers and ISL1-positive cells in early human and mouse forebrain.** *A*, *B*: Double immunofluorescent staining for TUJ1 and RELN in WPC7 (*A*) and WPC8 (*B*) human forebrain coronal sections. RELN-positive Cajal-Retzius cells are positive for TUJ1in the neocortex (Ncx) (*A′*–*A‴* and *B′*–*B‴*). There is abundant RELN-positive signal in the ventral telencephalon (vTel) at WPC7 and WPC8. Rare RELN-positive cells are visualized in the cortical hem at WPC7 and many more at WPC8. *A′*–*A‴* correspond to selected area in *A* and *B′*–*B‴* to boxed area in *B*. *C*–*F*: At WPC7, human coronal sections at rostral (*C*) and caudal (*D*) levels, stained for NF-160. Dense fiber fascicles are distributed in the PP of the neocortex (Ncx), forming the primordial plexiform layer, and extend in the ventral telencephalon at more caudal levels. NF-160–positive fibers also run between the prethalamus (pTh) and the dorsal thalamus (dTh), and in hypothalamus (Hyp) (*D*). NF-160 immunostaining of E12.5 mouse forebrain shows similar fiber patterns (*E*, *F*). *G*–*J*: ISL1 immunostaining in WPC7 discloses a pool of ISL1-positive cells in the ventral telencephalon, in the region where the future corticofugal axons travel (*G*), and another population of ISL1-positive cells in the prethalamus more caudally (pTh, *H*). A similar distribution of ISL1-positive cells is present in E12.5 mouse (*I*, *J*). LV, lateral ventricle.

positive cells in the ventral telencephalon and the prethalamus sent pioneer axons across the DTJ at E12.5 to guide later developing thalamocortical axons (Feng et al. 2016). To assess whether similar events may occur during human development, we labeled ISL1-positive cells using anti-ISL1 antibodies, and early fibers using anti-neurofilament NF-160 antibodies, and performed DiI tracing experiments. At rostral levels, NF-positive fibers were distributed along the pial surface of the telencephalon and in the ventral region of the ventral telencephalon (Fig. 6C). At caudal levels, intensely stained axons extended from the prethalamus to the dorsal thalamus and the hypothalamus (Fig. 6D). The distribution of these early fibers was similar in human and mice (Fig. 6E,F). ISL1-positive cells were present in the human forebrain (Fig. 6G,H) like in mice (Fig. 6I,J). At rostral levels, they were concentrated in the ventral telencephalon, an area where thalamocortical and corticothalamic axons grow at later stages. ISL1-positive cells were present in the prethalamus at more caudal levels, as well as in some unidentified hypothalamic areas.

To assess whether pioneer fibers crossed the DTJ prior to the arrival of thalamocortical axons, we inserted DiI crystals in the prethalamus or the ventral telencephalon in thick WPC7 vibratome sections, coupled with anti-ISL1 immunostaining. Upon DiI implantation in prethalamus, where ISL1-positive cells

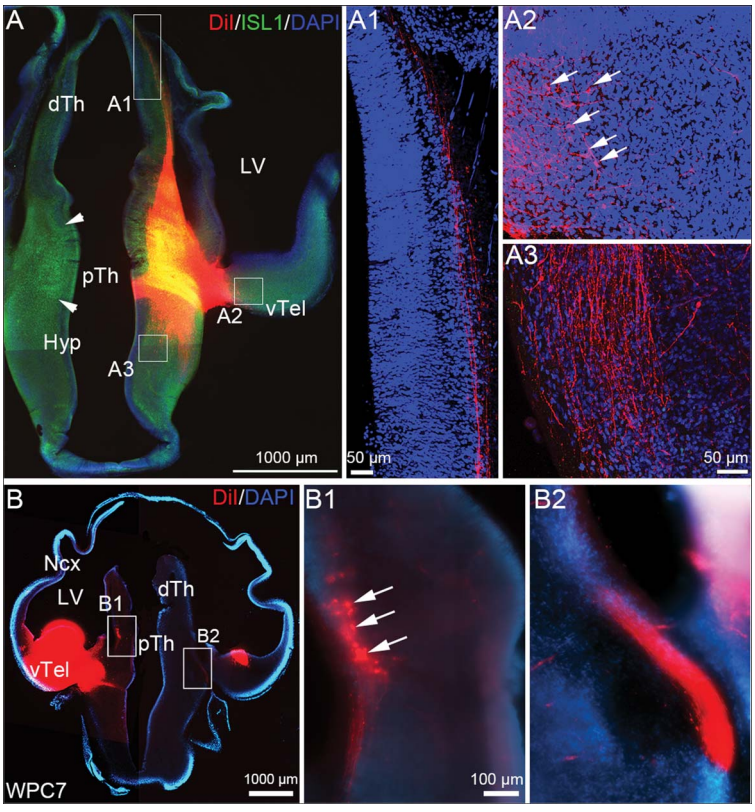

Figure 7. **Pioneer fibers bridge the DTJ in the early forebrain.** *A*: In WPC7 vibratome sections, DiI implantation in the prethalamus (pTh), where ISL1-positive cells are abundant (green, arrowheads), label early fibers in the dorsal thalamus (dTh), the ventral telencephalon (vTel) and the hypothalamus (Hyp). Whereas fibers but no cell bodies are back-labeled in dTh (*A1*) and Hyp (*A3*), anterogradely labeled pioneer axons and retrogradely labeled cells are found in vTel (*A2*, arrows). *A1*–*A3* are selected areas from *A*, as indicated. *B*: DiI implantation in vTel back-labels cell bodies in the pTh (*B1*, arrows), and anterogradely labels pioneer axons across the DTJ (*B2*). *B1* and *B2* are high magnifications of insets indicated in *B*. LV, lateral ventricle; Ncx, neocortex.

are abundant, labeled fibers were traced in the dorsal thalamus, the ventral telencephalon, and the hypothalamus (Fig. 7A). No cell bodies were labeled in dorsal thalamus (Fig. 7A1), indicating that pioneer fibers projected to the dorsal thalamus before thalamic neurons sent axons to the prethalamus. In the ventral telencephalon, both anterogradely labeled axons and retrogradely labeled cell bodies were seen (Fig. 7A2). DiI implantation in the ventral telencephalon resulted in anterograde labeling of axons across the DTJ and in retrograde labeling of cell bodies in the prethalamus (Fig. 7B,B1,B2). Taken together, those observations suggest that pioneer axons from the prethalamus and the ventral telencephalon do cross the DTJ in opposite direction before dorsal thalamic axons develop and that pioneer axons from the prethalamus project to the dorsal thalamic region.

Another key boundary is the PSPB, where early corticofugal axons leave the dorsal telencephalon to enter the future internal capsule (Wang et al. 2010). In mice, Isl1-positive cells in the ventral telencephalon guide corticothalamic axons after they run across the PSPB (Zhou et al. 2008; Feng et al. 2016). At WPC8, when the first corticofugal axons cross that frontier and reach the ventral telencephalon (Garel and Lopez-Bendito 2014), the PSPB was clearly defined by the distribution of TBR2-positive intermediate cortical progenitors and TBR1-positive early subcortical plate and CP neurons (Fig. 8A). Using double immunofluorescent staining for ISL1 and NF, we found that NF-positive fibers were surrounded by and came in close contact with ISL1-positive cells in the ventral telencephalon (Fig. 8B). To define that relationship further, we implanted DiI in the neocortex, coupled with anti-ISL1 immunostaining (Fig. 8C). In the ventral telencephalon, a stream of ISL1-positive cells was observed, and DiI-labeled corticofugal axons crossed the PSPB and ran along them. A few ventral telencephalic cells labeled with DiI were also positive for ISL1 (Fig. 8C′–C‴), indicating that they contributed pioneer axons across the PSPB and therefore might assist in the guidance of corticofugal axons (Fig. 8D,E).

In mice, Celsr3 and Fzd3 play critical roles in early brain wiring (Zhou et al. 2008; Tissir and Goffinet 2013; Chai et al. 2015). In the forebrain, inactivation of Celsr3 or Fzd3 in Isl1-positive cells hampers the formation of an early scaffold, which then perturbs the guidance of thalamocortical projections (Chai et al. 2014; Hua et al. 2014; Feng et al. 2016). To assess whether a similar mechanism operates in human, we compared CELSR3 and FZD3 mRNA expression at WPC6 and WPC8, with that in mice at E12.5 and E14.5. At WPC6, CELSR3 signal was concentrated in the ventral telencephalon where ISL1-positive cells were located as described above, whereas the signal in the neocortex was weak (Fig. 9A,B), like in mice at E12.5 (Fig. 9A′,B′). Expression of FZD3 was wider than that of CELSR3, extending throughout the entire forebrain (Fig. 9C,C′,D,D′). At WPC8, the CELSR3 signal became significant in the neocortex, mainly in the presubplate layer (Alzu'bi et al. 2019); it extended into the ventral telencephalon, but remained absent from all ventricular zones in cortex or ganglionic eminences (Fig. 9E), like in E14.5 mouse (Fig. 9E′), in accord with expression in postmi-

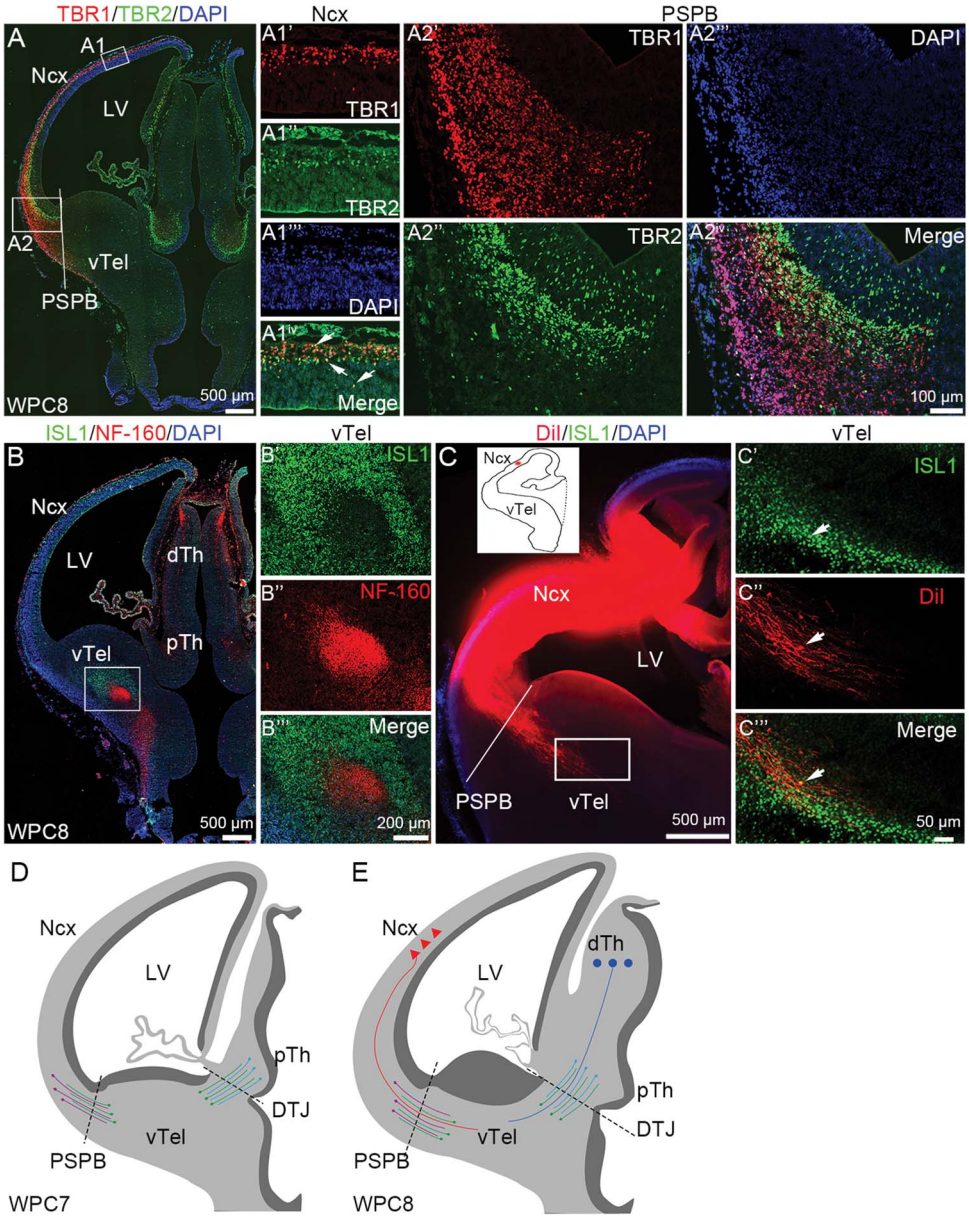

Figure 8. **Interaction between ISL1-positive cells and growing corticofugal axons.** *A*: Double immunofluorescence for TBR2 to label intermediate progenitors (green) and TBR1 to label early neurons (red) at WPC8. In the neocortical region (Ncx), TBR1-positive cells are in the subcortical plate and the incipient CP (*A1′*), whereas TBR2-positive intermediate progenitors are found deeper (*A1″*). A few cells are positive for both markers ($A1^{iv}$, arrows). This relative distribution is maintained in the region of the PSPB, although with less segregation and some mixing of both populations (*A2′*–$A2^{iv}$). *B*: Double immunofluorescent staining at WPC8, showing NF-160-positive fibers surrounded by ISL1-positive cells in ventral telencephalon (vTel; *B′*–*B‴*, area boxed in *B*). *C*: DiI implantation combined with ISL1 immunofluorescence at WPC8. Corticofugal axons cross the PSPB, enter and grow in vTel, closely opposed to the stream of ISL1-positive cells, some of which are retrogradely labeled (arrows in *C′*–*C‴*, area boxed in *C*). The drawing in *C* shows DiI implantation site in the Ncx. *D*, *E*: Schema to illustrate the formation of axonal scaffolds. At WPC7 (*D*), prior to growth of corticofugal and thalamic axons, pioneer neurons form reciprocal axonal scaffolds across the pallial-subpallial boundary (PSPB) and the diencephalon-telencephalon junction (DTJ). At WPC8 (*E*), corticofugal axons (red) and thalamic axons (blue) cross the PSPB and the DTJ along axonal scaffolds to invade the ventral telencephalon (vTel). Ncx, neocortex; LV, lateral ventricle; dTh, dorsal thalamus; pTh, prethalamus.

totic neurons and not in progenitor cells (Tissir et al. 2005). At caudal levels, the CELSR3 signal formed a stream across the DTJ, from the ventral telencephalon to the prethalamus in both species (Fig. 9F,F′), in a pattern similar to the bridge visible upon DiI tracing (Fig. 7). In addition, CELSR3 was robustly expressed in postmitotic cells in the dorsal thalamus, hypothalamus, and neocortex (Fig. 9F,F′). FZD3 expression overlapped with that of CELSR3 in postmitotic neurons in almost all regions, but, contrary to CELSR3, FZD3 was heavily expressed in ventricular zones along lateral and third ventricles in both species (Fig. 9G,H,G′,H′), showing that human FZD3 is expressed in both proliferating cells and postmitotic neurons (Wang et al. 2002). Thus, CELSR3 and FZD3 are highly expressed in the human embryonic forebrain, like in mice (Tissir et al. 2002), suggesting that they assume comparable functions during forebrain wiring.

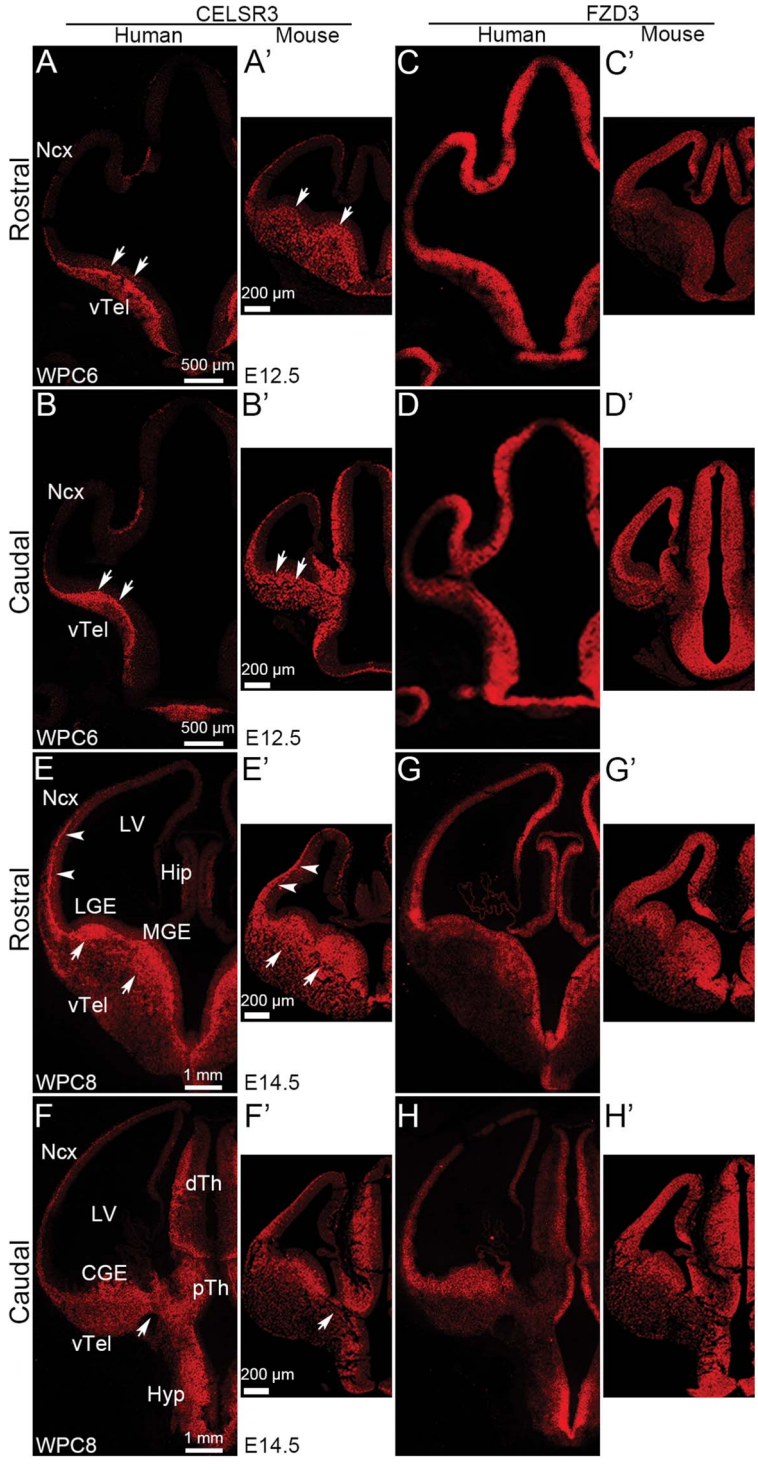

Figure 9. **CELSR3 and FZD3 mRNA expression.** *A–D*: At WPC6, CELSR3 in situ hybridization using RNAscope (*A*, *B*) shows strong signal in the ventral telencephalon (vTel, indicated by arrows), with almost no signal in cortex (Ncx); signal is absent from ventricular zones. The FZD3 signal (*C*, *D*) is more widely distributed and includes ventricular zones. Comparable expression patterns are shown in E12.5 mouse for CELSR3 (*A′*, *B′*; indicated by arrows) and FZD3 (*C′*, *D′*). *E–H*: At WPC8, CELSR3 signal (*E*, *F*) is present in the presubplate layer of cortex (Ncx; arrowheads in *E*), the vTel (arrows in *E*), and the diencephalon (dorsal thalamus, dTh; prethalamus, pTh; and Hyp), but not detected in ventricular zones. At caudal level (*F*) CELSR3-positive cells form a stream across the DTJ from the vTel to the pTh (arrow in *F*). The expression of FZD3 (*G*, *H*) is similar to that of CELSR3, except that it includes and is very high in ventricular zones. Similar expression patterns are found in mouse for CELSR3 (*E′*, *F′*) and FZD3 (*G′*, *H′*) at E14.5. OV, optic vesicle; LV, lateral ventricle; Hip, hippocampus; LGE, lateral ganglionic eminence; MGE, medial ganglionic eminence; CGE, caudal ganglionic eminence.

Discussion

The main observations in our study that we shall discuss briefly concern the following: 1) early telencephalic neurogenesis and formation of precocious neurons; 2) origin of Cajal-Retzius cells at the PP stage; and 3) the formation of a loose network of pioneer neurons and a scaffold of early axons at the PP stage.

Early Telencephalic Neurogenesis

At the NE stage, when hemispheres are not yet fully shaped and a superventricle precedes lateral ventricles, expression of PAX6 matched the well-known protomap, which was even more evident at the PP stage (Clowry et al. 2018). Expression of PH3 and Ki67 confirmed that the VZ was mostly populated by dividing neural progenitors (Carney et al. 2007; Florio and Huttner 2014). Somewhat unexpectedly, a significant number of cells in the external tier of the telencephalic wall expressed TBR2, a canonical marker of intermediate progenitor cells, and a small fraction of them were positive for the cell division marker Ki67. If cells that co-express TBR2 and Ki67 indeed correspond to intermediate progenitors, some indirect neurogenesis may occur at earlier stages of cortical neurogenesis than what is usually considered. In addition, the co-expression of TBR2 and TBR1 in a significant number of cells indicates that TBR2 expression might not be strictly restricted to intermediate progenitor cells at the NE stage and that a sequence of expression of TBR2 followed by TBR1 may be part of a program for formation of early neurons during direct neurogenesis. Data published in rodents are compatible with this view (Englund et al. 2005).

Precocious Neurons in the Early Telencephalic Wall

A minor yet significant number of TUJ1-positive neuronal cells were present in the external position, in which region DCX, a marker of immature migrating neurons, showed a similar expression pattern. Some DCX and Calbindin-positive precious neurons were present in a small dorsal–medial region. Immature TBR1-positive neurons were presumably generated from PAX6 progenitors and engaged in migration to the future PP. At more basal–ventral levels, in the region adjacent to the OLP, TUJ1 and DCX-positive precocious neurons seemed in continuity with a stream of TUJ1, Calretinin and DCX-positive cells of the OLP. Some of those cells expressed GnRH at WPC6, suggesting that they were similar to the early GnRH-positive cells generated in the OLP, perhaps with contribution from the neural crest (Suzuki and Osumi 2015) and destined to the preoptic area and future hypothalamus (Schwanzel-Fukuda et al. 1996; Casoni et al. 2016). Precocious cells at WPC5 did not express RELN or GAD65, a marker of an early tangential network that may guide growing axons (Garcia-Pena et al. 2014).

Given limitations inherent to work with human embryos, such as imperfect tissue preservation and fixation, the consistent localization of TUJ1 and GnRH suggests strongly that early neurons, some of which express GnRH, are generated in the OLP and migrate as a stream or "migratory mass" (Suzuki and Osumi 2015) to the incipient forebrain. This migratory stream likely corresponds to the terminal nerve, which is well defined in fish (Koide et al. 2018) but more elusive in mice (Taroc et al. 2017) and human (Fuller and Burger 1990; Vilensky 2014). Thus, our work indicates the presence of two precocious neurons in the neuroepithelial marginal zone. A first population derives from the local neuroepithelium, and a second may originate in the OLP. These precocious cells look reminiscent of the "predecessor neurons" described previously (Bystron et al. 2005; Bystron et al. 2008), which were shown to migrate tangentially from basal areas. As far as we know, a local origin of precocious neurons in the dorsal telencephalic neuroepithelium was not documented before. In the absence of molecular and lineage markers, the fate and function of precocious telencephalic neurons remain to be ascertained further.

Cajal-Retzius Cells and Reelin

The first RELN expressing cells were seen at WPC6–7, when abundant RELN-positive cells were scattered and seemed to originate from the area around the anti-hem or the region where DBX1-positive progenitors are described in ventral pallial and septal areas (Bielle et al. 2005). At those early stages, very few if any RELN-positive cells were found in the cortical hem. By contrast, at WPC8, abundant RELN-positive cells were found in the ventral telencephalon and the cortical marginal zones, as well as in the region of the medial cortical hem. This confirms that hem-derived Cajal-Retzius cells are generated later and/or initiate RELN expression later than those stemming from the anti-hem region. This temporal distinction is possible due to the protracted sequence of human development, whereas it is less well defined in mice, where events occur much faster (Meyer et al. 2000; Garcia-Moreno et al. 2007). A previous study showed the presence of radial streams of RELN-positive cells in the neuroepithelium at WPC6–7 (Meyer et al. 2000). The reason why those structures could not be seen in our material is unclear. At early stages, Cajal-Retzius cells are located close to the external limiting membrane and will migrate to deeper level in the marginal zone only later. Like in mice, RELN is not detected in PP pioneer neurons, which are located deeper in the marginal zone and are generated in the VZ locally and migrate radially. This confirms that Cajal-Retzius cells and pioneer PP neurons differ in terms of origin, migration, and gene expression and correspond to two different populations.

Pioneer PP Neurons and the Axonal Scaffold

At WPC6 and 7, the PP stage, developmental events in the human forebrain are grossly similar to those in mice and other mammals (Larroche 1981; Marin-Padilla 1983; Choi 1988; Letinic and Kostovic 1996; Zecevic et al. 1999; Meyer et al. 2000; Molnar and Clowry 2012). This was confirmed by in situ hybridization with a series of areal markers in addition to PAX6 and MASH1 that we used here (Bayatti et al. 2008; Ip et al. 2010; Alzu'bi, et al. 2017a; Clowry et al. 2018). Inasmuch as these aspects have been considered extensively elsewhere, we shall focus our discussion on our most original data, namely, the presence of early pioneer neurons and their axons, which precede and presumably guide the later growth of cortical and thalamic axons in the internal capsule.

A role for subplate neurons in guiding thalamocortical connections through the PSPB was demonstrated long ago in rodents and carnivores (McConnell et al. 1989; Ghosh et al. 1990; Allendoerfer and Shatz 1994; Molnar et al. 1998b). In parallel, studies in rodents showed the role of intermediate targets in corticothalamic and thalamocortical pathfinding (Deng and Elberger 2003), and investigations on the development of the internal capsule and reticular thalamic areas, which now would be considered as prethalamus, pointed to their role in guiding dorsal thalamic axons through the DTJ and ventral telencephalon (Molnar and Blakemore 1991; Mitrofanis and

Guillery 1993; Molnar et al. 1998a; Lopez-Bendito and Molnar 2003).

In contrast to cellular events that are reasonably well understood, molecular mechanisms remain more elusive. Neuregulin-1 was shown to assist the progression of thalamic axons in the ventral telencephalic corridor (Lopez-Bendito et al. 2006). Thalamocortical wiring anomalies were attributed to defective signaling by some Semaphorins (Bagnard et al. 2001; Lett et al. 2009), by ROBO/Slit (Andrews et al. 2006), as well as Ephrins/EPH (Dufour et al. 2003), reviewed in Molnar et al. (2012). More dramatic forebrain wiring defects were observed in mice with inactivation of Fzd3 (Wang et al. 2002; Hua et al. 2014) and Celsr3 (Tissir et al. 2005; Zhou et al. 2008; Tissir and Goffinet 2013), as well as Linx (aka Islr2) (Mandai et al. 2014) and Phr1 (aka MYCBP2) (Bloom et al. 2007). Studies of conditional Celsr3 and Fzd3 mutant mice showed that expression in some early guidepost cells, particularly Isl1-positive cells in ventral telencephalon, was required for thalamocortical wiring (Zhou et al. 2008; Hua et al. 2014). This led to the view that Celsr3 and Fzd3 regulate the formation of a scaffold of pioneer neurons and axons that are distributed from prethalamus to ventral telencephalon and cortical presubplate and pave the way for subsequent fibers from the cortical plate and thalamus (Feng et al. 2016). Our observations on the expression of CELSR3, FZD3, and ISL1 and our DiI tracing results clearly support that mechanism and suggest that it plays an important role in humans like in mice (summarized in Fig. 8*D*,*E*).

Funding

National Natural Science Foundation of China (31771133 and 31811530148, L. Zhou; 31671067 and U1801287, Y. Qu); Key Project of Natural Science Foundation of Guangdong province (1614050000335, L. Zhou); Programme of Introducing Talents of Discipline to Universities (B14036); Guangdong Natural Science Funds for Distinguished Young Scholars (2016A030306001, Y. Qu); Guangdong Province Special Support Program (2015TQ01R837, Y. Qu); Special Grants from the Guangzhou Pearl River Young Talents of Science and Technology (20160010023, Y. QU); and the fund from Guangzhou Women and Children's Medical Center/Guangzhou Institute of Pediatrics (IP-2018-016, T. Zhao).

Notes

We wish to thank the patients who gave their informed consent, and attending physicians and medical staff, Paolo Giacobini (INSERM, Lille), Lut Arckens and Eve Seuntjens (Katholiek Univ. Leuven) for providing GnRH antibodies, and Panpan Yu for critical comments. *Conflict of Interest*: None declared.

References

Al-Jaberi N, Lindsay S, Sarma S, Bayatti N, Clowry GJ. 2015. The early fetal development of human neocortical GABAergic interneurons. *Cereb Cortex*. 25:631–645.

Allendoerfer KL, Shatz CJ. 1994. The subplate, a transient neocortical structure: its role in the development of connections between thalamus and cortex. *Annu Rev Neurosci*. 17:185–218.

Alzu'bi A, Homman-Ludiye J, Bourne JA, Clowry GJ. 2019. Thalamocortical afferents innervate the cortical subplate much earlier in development in primate than in rodent. *Cereb Cortex*. 29:1706–1718.

Alzu'bi A, Lindsay S, Kerwin J, Looi SJ, Khalil F, Clowry GJ. 2017a. Distinct cortical and sub-cortical neurogenic domains for GABAergic interneuron precursor transcription factors NKX2.1, OLIG2 and COUP-TFII in early fetal human telencephalon. *Brain Struct Funct*. 222:2309–2328.

Alzu'bi A, Lindsay SJ, Harkin LF, McIntyre J, Lisgo SN, Clowry GJ. 2017b. The transcription factors COUP-TFI and COUP-TFII have distinct roles in arealisation and GABAergic interneuron specification in the early human fetal telencephalon. *Cereb Cortex*. 27:4971–4987.

Andrews W, Liapi A, Plachez C, Camurri L, Zhang J, Mori S, Murakami F, Parnavelas JG, Sundaresan V, Richards LJ. 2006. Robo1 regulates the development of major axon tracts and interneuron migration in the forebrain. *Development*. 133:2243–2252.

Arnold SJ, Huang GJ, Cheung AF, Era T, Nishikawa S, Bikoff EK, Molnar Z, Robertson EJ, Groszer M. 2008. The T-box transcription factor Eomes/Tbr2 regulates neurogenesis in the cortical subventricular zone. *Genes Dev*. 22:2479–2484.

Bagnard D, Chounlamountri N, Puschel AW, Bolz J. 2001. Axonal surface molecules act in combination with semaphorin 3a during the establishment of corticothalamic projections. *Cereb Cortex*. 11:278–285.

Bayatti N, Moss JA, Sun L, Ambrose P, Ward JF, Lindsay S, Clowry GJ. 2008. A molecular neuroanatomical study of the developing human neocortex from 8 to 17 postconceptional weeks revealing the early differentiation of the subplate and subventricular zone. *Cereb Cortex*. 18:1536–1548.

Bayer SA, Altman J. 2002. *Atlas of human central nervous system development*. Boca Raton: CRC Press.

de Bergeyck V, Naerhuyzen B, Goffinet AM, Lambert de Rouvroit C. 1998. A panel of monoclonal antibodies against reelin, the extracellular matrix protein defective in reeler mutant mice. *J Neurosci Methods*. 82:17–24.

Bielle F, Griveau A, Narboux-Neme N, Vigneau S, Sigrist M, Arber S, Wassef M, Pierani A. 2005. Multiple origins of Cajal–Retzius cells at the borders of the developing pallium. *Nat Neurosci*. 8:1002–1012.

Bloom AJ, Miller BR, Sanes JR, DiAntonio A. 2007. The requirement for Phr1 in CNS axon tract formation reveals the corticostriatal boundary as a choice point for cortical axons. *Genes Dev*. 21:2593–2606.

Butler AB, Hodos W. 2005. *Comparative vertebrate neuroanatomy: evolution and adaptation*. Hoboken, N.J: Wiley-Interscience.

Bystron I, Blakemore C, Rakic P. 2008. Development of the human cerebral cortex: Boulder Committee revisited. *Nat Rev Neurosci*. 9:110–122.

Bystron I, Molnar Z, Otellin V, Blakemore C. 2005. Tangential networks of precocious neurons and early axonal outgrowth in the embryonic human forebrain. *J Neurosci*. 25:2781–2792.

Bystron I, Rakic P, Molnar Z, Blakemore C. 2006. The first neurons of the human cerebral cortex. *Nat Neurosci*. 9:880–886.

Carney RS, Bystron I, Lopez-Bendito G, Molnar Z. 2007. Comparative analysis of extra-ventricular mitoses at early stages of cortical development in rat and human. *Brain Struct Funct*. 212:37–54.

Casarosa S, Fode C, Guillemot F. 1999. Mash1 regulates neurogenesis in the ventral telencephalon. *Development*. 126:525–534.

Casoni F, Malone SA, Belle M, Luzzati F, Collier F, Allet C, Hrabovszky E, Rasika S, Prevot V, Chedotal A *et al*. 2016. Development of the neurons controlling fertility in humans: new insights from 3D imaging and transparent fetal brains. *Development*. 143:3969–3981.

Chai G, Goffinet AM, Tissir F. 2015. Celsr3 and Fzd3 in axon guidance. *Int J Biochem Cell Biol*. 64:11–14.
Chai G, Zhou L, Manto M, Helmbacher F, Clotman F, Goffinet AM, Tissir F. 2014. Celsr3 is required in motor neurons to steer their axons in the hindlimb. *Nat Neurosci*. 17:1171–1179.
Choi BH. 1988. Developmental events during the early stages of cerebral cortical neurogenesis in man. A correlative light, electron microscopic, immunohistochemical and Golgi study. *Acta Neuropathol*. 75:441–447.
Clowry G, Molnar Z, Rakic P. 2010. Renewed focus on the developing human neocortex. *J Anat*. 217:276–288.
Clowry GJ, Alzu'bi A, Harkin LF, Sarma S, Kerwin J, Lindsay SJ. 2018. Charting the protomap of the human telencephalon. *Semin Cell Dev Biol*. 76:3–14.
Dehay C, Kennedy H, Kosik KS. 2015. The outer subventricular zone and primate-specific cortical complexification. *Neuron*. 85:683–694.
Deng J, Elberger AJ. 2003. Corticothalamic and thalamocortical pathfinding in the mouse: dependence on intermediate targets and guidance axis. *Anat Embryol (Berl)*. 207:177–192.
Di Lullo E, Kriegstein AR. 2017. The use of brain organoids to investigate neural development and disease. *Nat Rev Neurosci*. 18:573–584.
Dufour A, Seibt J, Passante L, Depaepe V, Ciossek T, Frisen J, Kullander K, Flanagan JG, Polleux F, Vanderhaeghen P. 2003. Area specificity and topography of thalamocortical projections are controlled by ephrin/Eph genes. *Neuron*. 39:453–465.
Englund C, Fink A, Lau C, Pham D, Daza RA, Bulfone A, Kowalczyk T, Hevner RF. 2005. Pax6, Tbr2, and Tbr1 are expressed sequentially by radial glia, intermediate progenitor cells, and postmitotic neurons in developing neocortex. *J Neurosci*. 25:247–251.
Feng J, Xian Q, Guan T, Hu J, Wang M, Huang Y, So KF, Evans SM, Chai G, Goffinet AM *et al*. 2016. Celsr3 and Fzd3 organize a pioneer neuron scaffold to steer growing thalamocortical axons. *Cereb Cortex*. 26:3323–3334.
Fernandez AS, Pieau C, Reperant J, Boncinelli E, Wassef M. 1998. Expression of the Emx-1 and Dlx-1 homeobox genes define three molecularly distinct domains in the telencephalon of mouse, chick, turtle and frog embryos: implications for the evolution of telencephalic subdivisions in amniotes. *Development*. 125:2099–2111.
Florio M, Borrell V, Huttner WB. 2017. Human-specific genomic signatures of neocortical expansion. *Curr Opin Neurobiol*. 42:33–44.
Florio M, Huttner WB. 2014. Neural progenitors, neurogenesis and the evolution of the neocortex. *Development*. 141:2182–2194.
Fuller GN, Burger PC. 1990. Nervus terminalis (cranial nerve zero) in the adult human. *Clin Neuropathol*. 9:279–283.
Garcia-Moreno F, Lopez-Mascaraque L, De Carlos JA. 2007. Origins and migratory routes of murine Cajal-Retzius cells. *J Comp Neurol*. 500:419–432.
Garcia-Pena CM, Kim M, Frade-Perez D, Avila-Gonzalez D, Tellez E, Mastick GS, Tamariz E, Varela-Echavarria A. 2014. Ascending midbrain dopaminergic axons require descending GAD65 axon fascicles for normal pathfinding. *Front Neuroanat*. 8:43.
Garel S, Lopez-Bendito G. 2014. Inputs from the thalamocortical system on axon pathfinding mechanisms. *Curr Opin Neurobiol*. 27:143–150.
Ghosh A, Antonini A, McConnell SK, Shatz CJ. 1990. Requirement for subplate neurons in the formation of thalamocortical connections. *Nature*. 347:179–181.
Gonzalez-Gomez M, Meyer G. 2014. Dynamic expression of calretinin in embryonic and early fetal human cortex. *Front Neuroanat*. 8:41.
Hern WM. 1984. Correlation of fetal age and measurements between 10 and 26 weeks of gestation. *Obstet Gynecol*. 63:26–32.
Hoch RV, Rubenstein JL, Pleasure S. 2009. Genes and signaling events that establish regional patterning of the mammalian forebrain. *Semin Cell Dev Biol*. 20:378–386.
Hua ZL, Jeon S, Caterina MJ, Nathans J. 2014. Frizzled3 is required for the development of multiple axon tracts in the mouse central nervous system. *Proc Natl Acad Sci U S A*. 111:E3005–E3014.
Ip BK, Wappler I, Peters H, Lindsay S, Clowry GJ, Bayatti N. 2010. Investigating gradients of gene expression involved in early human cortical development. *J Anat*. 217:300–311.
Koide T, Yabuki Y, Yoshihara Y. 2018. Terminal nerve GnRH3 neurons mediate slow avoidance of carbon dioxide in larval zebrafish. *Cell Rep*. 22:1115–1123.
LaMonica BE, Lui JH, Wang X, Kriegstein AR. 2012. OSVZ progenitors in the human cortex: an updated perspective on neurodevelopmental disease. *Curr Opin Neurobiol*. 22: 747–753.
Larroche JC. 1981. The marginal layer in the neocortex of a 7 week-old human embryo. A light and electron microscopic study. *Anat Embryol (Berl)*. 162:301–312.
Letinic K, Kostovic I. 1996. Transient neuronal population of the internal capsule in the developing human cerebrum. *Neuroreport*. 7:2159–2162.
Lett RL, Wang W, O'Connor TP. 2009. Semaphorin 5B is a novel inhibitory cue for corticofugal axons. *Cereb Cortex*. 19:1408–1421.
Lopez-Bendito G, Cautinat A, Sanchez JA, Bielle F, Flames N, Garratt AN, Talmage DA, Role LW, Charnay P, Marin O *et al*. 2006. Tangential neuronal migration controls axon guidance: a role for neuregulin-1 in thalamocortical axon navigation. *Cell*. 125:127–142.
Lopez-Bendito G, Molnar Z. 2003. Thalamocortical development: how are we going to get there. *Nat Rev Neurosci*. 4:276–289.
Mandai K, Reimert DV, Ginty DD. 2014. Linx mediates interaxonal interactions and formation of the internal capsule. *Neuron*. 83:93–103.
Marin-Padilla M. 1983. Structural organization of the human cerebral cortex prior to the appearance of the cortical plate. *Anat Embryol (Berl)*. 168:21–40.
Marin O. 2013. Cellular and molecular mechanisms controlling the migration of neocortical interneurons. *Eur J Neurosci*. 38:2019–2029.
McConnell SK, Ghosh A, Shatz CJ. 1989. Subplate neurons pioneer the first axon pathway from the cerebral cortex. *Science*. 245:978–982.
Metin C, Godement P. 1996. The ganglionic eminence may be an intermediate target for corticofugal and thalamocortical axons. *J Neurosci*. 16:3219–3235.
Meyer G. 2001. Human neocortical development: the importance of embryonic and early fetal events. *Neuroscientist*. 7:303–314.
Meyer G, Perez-Garcia CG, Gleeson JG. 2002. Selective expression of doublecortin and LIS1 in developing human cortex suggests unique modes of neuronal movement. *Cereb Cortex*. 12:1225–1236.
Meyer G, Schaaps JP, Moreau L, Goffinet AM. 2000. Embryonic and early fetal development of the human neocortex. *J Neurosci*. 20:1858–1868.

Mitrofanis J, Guillery RW. 1993. New views of the thalamic reticular nucleus in the adult and the developing brain. *Trends Neurosci*. 16:240–245.

Molnar Z, Adams R, Blakemore C. 1998a. Mechanisms underlying the early establishment of thalamocortical connections in the rat. *J Neurosci*. 18:5723–5745.

Molnar Z, Adams R, Goffinet AM, Blakemore C. 1998b. The role of the first postmitotic cortical cells in the development of thalamocortical innervation in the reeler mouse. *J Neurosci*. 18:5746–5765.

Molnar Z, Blakemore C. 1991. Lack of regional specificity for connections formed between thalamus and cortex in coculture. *Nature*. 351:475–477.

Molnar Z, Clowry G. 2012. Cerebral cortical development in rodents and primates. *Prog Brain Res*. 195:45–70.

Molnar Z, Cordery P. 1999. Connections between cells of the internal capsule, thalamus, and cerebral cortex in embryonic rat. *J Comp Neurol*. 413:1–25.

Molnar Z, Garel S, Lopez-Bendito G, Maness P, Price DJ. 2012. Mechanisms controlling the guidance of thalamocortical axons through the embryonic forebrain. *Eur J Neurosci*. 35:1573–1585.

O'Leary DD, Sahara S. 2008. Genetic regulation of arealization of the neocortex. *Curr Opin Neurobiol*. 18:90–100.

O'Rahilly R, Müller F. 2006. *The embryonic human brain: an atlas of developmental stages*. Hoboken, NJ: Wiley-Liss.

Ostrem B, Di Lullo E, Kriegstein A. 2017. oRGs and mitotic somal translocation—a role in development and disease. *Curr Opin Neurobiol*. 42:61–67.

Parnavelas JG. 2000. The origin and migration of cortical neurones: new vistas. *Trends Neurosci*. 23:126–131.

Pasca SP. 2018. The rise of three-dimensional human brain cultures. *Nature*. 553:437–445.

Pedraza M, Hoerder-Suabedissen A, Albert-Maestro MA, Molnar Z, De Carlos JA. 2014. Extracortical origin of some murine subplate cell populations. *Proc Natl Acad Sci U S A*. 111:8613–8618.

Puelles L. 2017. Comments on the updated tetrapartite pallium model in the mouse and Chick, featuring a homologous claustro-insular complex. *Brain Behav Evol*. 90:171–189.

Qu Y, Huang Y, Feng J, Alvarez-Bolado G, Grove EA, Yang Y, Tissir F, Zhou L, Goffinet AM. 2014. Genetic evidence that Celsr3 and Celsr2, together with Fzd3, regulate forebrain wiring in a Vangl-independent manner. *Proc Natl Acad Sci U S A*. 111:E2996–E3004.

Rakic P, Ayoub AE, Breunig JJ, Dominguez MH. 2009. Decision by division: making cortical maps. *Trends Neurosci*. 32:291–301.

Reillo I, Borrell V. 2012. Germinal zones in the developing cerebral cortex of ferret: ontogeny, cell cycle kinetics, and diversity of progenitors. *Cereb Cortex*. 22:2039–2054.

Schiffmann SN, Bernier B, Goffinet AM. 1997. Reelin mRNA expression during mouse brain development. *Eur J Neurosci*. 9:1055–1071.

Schwanzel-Fukuda M, Abraham S, Crossin KL, Edelman GM, Pfaff DW. 1992. Immunocytochemical demonstration of neural cell adhesion molecule (NCAM) along the migration route of luteinizing hormone-releasing hormone (LHRH) neurons in mice. *J Comp Neurol*. 321:1–18.

Schwanzel-Fukuda M, Crossin KL, Pfaff DW, Bouloux PM, Hardelin JP, Petit C. 1996. Migration of luteinizing hormone-releasing hormone (LHRH) neurons in early human embryos. *J Comp Neurol*. 366:547–557.

Smart IH, Dehay C, Giroud P, Berland M, Kennedy H. 2002. Unique morphological features of the proliferative zones and postmitotic compartments of the neural epithelium giving rise to striate and extrastriate cortex in the monkey. *Cereb Cortex*. 12:37–53.

Super H, Soriano E, Uylings HB. 1998. The functions of the preplate in development and evolution of the neocortex and hippocampus. *Brain Res Brain Res Rev*. 27:40–64.

Suzuki IK, Vanderhaeghen P. 2015. Is this a brain which I see before me? Modeling human neural development with pluripotent stem cells. *Development*. 142:3138–3150.

Suzuki J, Osumi N. 2015. Neural crest and placode contributions to olfactory development. *Curr Top Dev Biol*. 111:351–374.

Taroc EZM, Prasad A, Lin JM, Forni PE. 2017. The terminal nerve plays a prominent role in GnRH-1 neuronal migration independent from proper olfactory and vomeronasal connections to the olfactory bulbs. *Biol Open*. 6:1552–1568.

Tissir F, Bar I, Jossin Y, De Backer O, Goffinet AM. 2005. Protocadherin Celsr3 is crucial in axonal tract development. *Nat Neurosci*. 8:451–457.

Tissir F, De-Backer O, Goffinet AM, Lambert de Rouvroit C. 2002. Developmental expression profiles of Celsr (Flamingo) genes in the mouse. *Mech Dev*. 112:157–160.

Tissir F, Goffinet AM. 2003. Reelin and brain development. *Nat Rev Neurosci*. 4:496–505.

Tissir F, Goffinet AM. 2013. Shaping the nervous system: role of the core planar cell polarity genes. *Nat Rev Neurosci*. 14:525–535.

Toresson H, Potter SS, Campbell K. 2000. Genetic control of dorsal-ventral identity in the telencephalon: opposing roles for Pax6 and Gsh2. *Development*. 127:4361–4371.

Vasistha NA, Garcia-Moreno F, Arora S, Cheung AF, Arnold SJ, Robertson EJ, Molnar Z. 2015. Cortical and clonal contribution of Tbr2 expressing progenitors in the developing mouse brain. *Cereb Cortex*. 25:3290–3302.

Vilensky JA. 2014. The neglected cranial nerve: nervus terminalis (cranial nerve N). *Clin Anat*. 27:46–53.

Walker TL, Yasuda T, Adams DJ, Bartlett PF. 2007. The doublecortin-expressing population in the developing and adult brain contains multipotential precursors in addition to neuronal-lineage cells. *J Neurosci*. 27:3734–3742.

Wang WZ, Hoerder-Suabedissen A, Oeschger FM, Bayatti N, Ip BK, Lindsay S, Supramaniam V, Srinivasan L, Rutherford M, Mollgard K *et al*. 2010. Subplate in the developing cortex of mouse and human. *J Anat*. 217:368–380.

Wang Y, Thekdi N, Smallwood PM, Macke JP, Nathans J. 2002. Frizzled-3 is required for the development of major fiber tracts in the rostral CNS. *J Neurosci*. 22:8563–8573.

Zecevic N, Milosevic A, Rakic S, Marin-Padilla M. 1999. Early development and composition of the human primordial plexiform layer: an immunohistochemical study. *J Comp Neurol*. 412:241–254.

Zhou L, Bar I, Achouri Y, Campbell K, De Backer O, Hebert JM, Jones K, Kessaris N, de Rouvroit CL, O'Leary D *et al*. 2008. Early forebrain wiring: genetic dissection using conditional Celsr3 mutant mice. *Science*. 320:946–949.